

A SM-like Higgs near 125 GeV in low energy SUSY: a comparative study for MSSM and NMSSM

Junjie Cao^{1,2}, Zhaoxia Heng¹, Jin Min Yang³, Yanming Zhang¹, Jingya Zhu³,

¹ *Department of Physics, Henan Normal University, Xinxiang 453007, China*

² *Center for High Energy Physics, Peking University, Beijing 100871, China*

³ *State Key Laboratory of Theoretical Physics,*

Institute of Theoretical Physics, Academia Sinica, Beijing 100190, China

Abstract

Motivated by the recent LHC hints of a Higgs boson around 125 GeV, we assume a SM-like Higgs with the mass 123-127 GeV and study its implication in low energy SUSY by comparing the MSSM and NMSSM. We consider various experimental constraints at 2σ level (including the muon $g-2$ and the dark matter relic density) and perform a comprehensive scan over the parameter space of each model. Then in the parameter space which is allowed by current experimental constraints and also predicts a SM-like Higgs in 123-127 GeV, we examine the properties of the sensitive parameters (like the top squark mass and the trilinear coupling A_t) and calculate the rates of the di-photon signal and the VV^* ($V = W, Z$) signals at the LHC. Our typical findings are: (i) In the MSSM the top squark and A_t must be large and thus incur some fine-tuning, which can be much ameliorated in the NMSSM; (ii) In the MSSM a light stau is needed to enhance the di-photon rate of the SM-like Higgs to exceed its SM prediction, while in the NMSSM the di-photon rate can be readily enhanced in several ways; (iii) In the MSSM the signal rates of $pp \rightarrow h \rightarrow VV^*$ at the LHC are never enhanced compared with their SM predictions, while in the NMSSM they may get enhanced significantly; (iv) A large part of the parameter space so far survived will be soon covered by the expected XENON100(2012) sensitivity (especially for the NMSSM).

PACS numbers:

I. INTRODUCTION

As the only missing particle in the Standard Model (SM), the Higgs boson is being intensively hunted at the LHC. Recently, both the ATLAS and CMS experiments have revealed hints of a Higgs particle around 125GeV [1, 2]. While such a Higgs mass can be well accommodated in the SM and the reported signal rates in several channels are also in agreement with the SM expectations after taking into account the large experimental uncertainty [3, 4] (albeit the central value of the observed di-photon rate is somewhat above the SM prediction), the low energy supersymmetry (SUSY) seems to be a better framework to account for such a Higgs. In low energy SUSY the SM-like Higgs mass is theoretically restricted in a narrow range and its di-photon rate at the LHC may exceed the SM prediction [5–7], both of which are welcomed by the LHC results.

However, as the most popular low energy SUSY model, the minimal supersymmetric standard model (MSSM) [8, 9] may have some tension to accommodate such a 125 GeV Higgs. As is well known, in the MSSM the SM-like Higgs mass is upper bounded by $M_Z \cos 2\beta$ at tree-level and to get a Higgs around 125GeV we need sizable top/stop loop contributions, which depend quartically on the top quark mass and logarithmically on the stop masses [10]. This will, on the one hand, impose rather tight constraint on the MSSM, and on the other hand, incur some fine-tuning [11]. Such a problem can be alleviated in the so-called next-to-minimal supersymmetric standard model (NMSSM) [12, 13], which is the simplest singlet extension of the MSSM with a scale invariant superpotential. In the NMSSM, due to the introduction of some new couplings in the superpotential, the SM-like Higgs mass gets additional contribution at tree-level and also may be further pushed up by the mixing effect in diagonalizing the mass matrix of the CP-even Higgs fields [14, 15]. As a result, a SM-like Higgs around 125GeV does not entail large loop contributions, which may thus ameliorate the fine-tuning problem [16].

In this work, motivated by the recent LHC results, we assume a SM-like Higgs boson in 123 – 127 GeV and study its implication in the MSSM and NMSSM. Different from recent studies in this direction [7, 14, 15, 17, 18], we scan the model parameters by considering various experimental constraints and perform a comparative study for the MSSM and NMSSM. We will investigate the features of the allowed parameter space in each model and particularly we pay more attention to the space of the NMSSM which may be dis-

inct from the MSSM. Noting the LHC experiments utilize the channels $pp \rightarrow h \rightarrow \gamma\gamma$, $pp \rightarrow h \rightarrow ZZ^* \rightarrow 4l$ and $pp \rightarrow h \rightarrow WW^* \rightarrow 2l\ 2\nu$ in searching for the Higgs boson [1, 2], we also study their normalized production rates defined as

$$\begin{aligned} R_{\gamma\gamma} &\equiv \sigma_{SUSY}(pp \rightarrow h \rightarrow \gamma\gamma)/\sigma_{SM}(pp \rightarrow h \rightarrow \gamma\gamma) \\ &\equiv C_{hgg}^2 C_{h\gamma\gamma}^2 \times \Gamma_{tot}(h_{SM})/\Gamma_{tot}(h), \end{aligned} \quad (1)$$

$$\begin{aligned} R_{VV} &\equiv \sigma_{SUSY}(pp \rightarrow h \rightarrow VV^*)/\sigma_{SM}(pp \rightarrow h \rightarrow VV^*) \\ &\equiv C_{hgg}^2 C_{hVV}^2 \times \Gamma_{tot}(h_{SM})/\Gamma_{tot}(h), \end{aligned} \quad (2)$$

where $V = W, Z$, and C_{hgg} , $C_{h\gamma\gamma}$ and C_{hVV} are respectively the rescaled couplings of the Higgs to gluons, photons and weak gauge bosons by their SM values. We are more interested in the case with $R_{\gamma\gamma} > 1$ because it is favored by current ATLAS and CMS results [1–3]. As will be shown below, this case usually predicts a slepton or a chargino lighter than 250 GeV.

This paper is organized as follows. In Sec. II, we recapitulate the characters of the Higgs mass in the models for better understanding our numerical results. In Sec. III, we perform a comprehensive scan over the parameter space of each model by imposing current experimental constraints and also by requiring a SM-like Higgs boson in 123 – 127 GeV. Then we scrutinize the properties of the surviving parameter space. Finally, we draw our conclusions in Sec. IV.

II. THE SM-LIKE HIGGS MASS IN THE MSSM AND NMSSM

In the MSSM, the Higgs sector consists of two doublet fields H_u and H_d , which after the electroweak symmetry breaking, result in five physical Higgs bosons: two CP-even scalars h and H , one CP-odd pseudoscalar A and a pair of charged scalars H^\pm [8]. Traditionally, such a Higgs sector is described by the ratio of the Higgs vacuum expectation values, $\tan\beta \equiv \frac{v_u}{v_d}$, and the mass of the pseudoscalar m_A . In most of the MSSM parameter space, the lightest Higgs boson h has largest coupling to vector bosons (i.e. the so-called SM-like Higgs boson), and for moderate $\tan\beta$ and large m_A its mass is given by [18]

$$m_h^2 \simeq M_Z^2 \cos^2 2\beta + \frac{3m_t^4}{4\pi^2 v^2} \ln \frac{M_S^2}{m_t^2} + \frac{3m_t^4}{4\pi^2 v^2} \frac{X_t^2}{M_S^2} \left(1 - \frac{X_t^2}{12M_S^2}\right), \quad (3)$$

where $v = 174$ GeV, $M_S = \sqrt{m_{\tilde{t}_1} m_{\tilde{t}_2}}$ with $m_{\tilde{t}_1}$ and $m_{\tilde{t}_2}$ being the stop masses, $X_t \equiv A_t - \mu \cot\beta$ with A_t denoting the trilinear Higgs-stop coupling and μ being the Higgsino

mass parameter. Obviously, the larger $\tan\beta$ or M_S is, the heavier h becomes, and for given M_S , m_h reaches its maximum when $X_t/M_S = \sqrt{6}$, which corresponds to the so-called m_h^{max} scenario.

About Eq.(3), three points should be noted [18]. The first is this equation is only valid for small splitting between $m_{\tilde{t}_1}$ and $m_{\tilde{t}_2}$. In case of large splitting, generally $X_t/M_S > \sqrt{6}$ is needed to maximize m_h . The second is m_h^2 in Eq.(3) is symmetric with respect to the sign of X_t . This behavior will be spoiled once higher order corrections are considered, and usually a larger m_h is achieved for positive $A_t M_3$ with M_3 being gluino soft breaking mass. And the last is in Eq.(3), we do not include the contributions from the sbottom and slepton sectors. Such contributions are negative and become significant only for large $\tan\beta$.

Compared with the MSSM, the Higgs sector in the NMSSM is rather complex, which can be seen from its superpotential and the corresponding soft-breaking terms given by [12]

$$W_{\text{NMSSM}} = W_F + \lambda \hat{H}_u \cdot \hat{H}_d \hat{S} + \frac{1}{3} \kappa \hat{S}^3, \quad (4)$$

$$V_{\text{soft}}^{\text{NMSSM}} = \tilde{m}_u^2 |H_u|^2 + \tilde{m}_d^2 |H_d|^2 + \tilde{m}_S^2 |S|^2 + (A_\lambda \lambda S H_u \cdot H_d + \frac{A_\kappa}{3} \kappa S^3 + h.c.). \quad (5)$$

Here W_F is the superpotential of the MSSM without the μ term, the dimensionless parameters λ and κ are the coefficients of the Higgs self couplings, and \tilde{m}_u , \tilde{m}_d , \tilde{m}_S , A_λ and A_κ are the soft-breaking parameters.

After the electroweak symmetry breaking, the three soft breaking masses squared for H_u , H_d and S can be expressed in terms of their VEVs (i.e. v_u , v_d and s) through the minimization conditions of the scalar potential. So in contrast to the MSSM where there are only two parameters in the Higgs sector, the Higgs sector of the NMSSM is described by six parameters [12]:

$$\lambda, \quad \kappa, \quad M_A^2 = \frac{2\mu(A_\lambda + \kappa s)}{\sin 2\beta}, \quad A_\kappa, \quad \tan\beta = \frac{v_u}{v_d}, \quad \mu = \lambda s. \quad (6)$$

The Higgs fields can be written in the following form:

$$H_1 = \begin{pmatrix} H^+ \\ \frac{S_1 + iP_1}{\sqrt{2}} \end{pmatrix}, \quad H_2 = \begin{pmatrix} G^+ \\ v + \frac{S_2 + iG^0}{\sqrt{2}} \end{pmatrix}, \quad H_3 = s + \frac{1}{\sqrt{2}} (S_3 + iP_2), \quad (7)$$

where $H_1 = \cos\beta H_u - \varepsilon \sin\beta H_d^*$, $H_2 = \sin\beta H_u + \varepsilon \cos\beta H_d^*$ with $\varepsilon_{12} = \varepsilon_{21} = -1$ and $\varepsilon_{11} = \varepsilon_{22} = 0$, G^+ and G^0 are Goldstone bosons and $v = \sqrt{v_u^2 + v_d^2}$. In the CP-conserving NMSSM, the fields S_1 , S_2 and S_3 mix to form three physical CP-even Higgs bosons, and P_1

and P_2 mix to form two physical CP-odd Higgs bosons. Obviously, the field H_2 corresponds to the SM Higgs field, and the scalar h with largest S_2 component is called the SM-like Higgs boson.

Under the basis (S_1, S_2, S_3) , the elements of the mass matrix for S_i fields at tree level are given by [15, 19]

$$\mathcal{M}_{11}^2 = M_A^2 + (m_Z^2 - \lambda^2 v^2) \sin^2 2\beta, \quad (8)$$

$$\mathcal{M}_{12}^2 = -\frac{1}{2}(m_Z^2 - \lambda^2 v^2) \sin 4\beta, \quad (9)$$

$$\mathcal{M}_{13}^2 = -(M_A^2 \sin 2\beta + \frac{2\kappa\mu^2}{\lambda}) \frac{\lambda v}{\mu} \cos 2\beta, \quad (10)$$

$$\mathcal{M}_{22}^2 = m_Z^2 \cos^2 2\beta + \lambda^2 v^2 \sin^2 2\beta, \quad (11)$$

$$\mathcal{M}_{23}^2 = 2\lambda\mu v \left[1 - \left(\frac{M_A \sin 2\beta}{2\mu} \right)^2 - \frac{\kappa}{2\lambda} \sin 2\beta \right], \quad (12)$$

$$\mathcal{M}_{33}^2 = \frac{1}{4}\lambda^2 v^2 \left(\frac{M_A \sin 2\beta}{\mu} \right)^2 + \frac{\kappa\mu}{\lambda} \left(A_\kappa + \frac{4\kappa\mu}{\lambda} \right) - \frac{1}{2}\lambda\kappa v^2 \sin 2\beta, \quad (13)$$

where \mathcal{M}_{22}^2 is nothing but m_h^2 at tree level without considering the mixing among S_i , and its second term $\lambda^2 v^2 \sin^2 2\beta$ originates from the coupling $\lambda \hat{H}_u \cdot \hat{H}_d \hat{S}$ in the superpotential. For such a complex matrix, it is useful to consider two scenarios for understanding the results:

- Scenario I: $\lambda, \kappa \rightarrow 0$ and μ is fixed. In this limit, since $\mathcal{M}_{13}^2, \mathcal{M}_{23}^2 \simeq 0$, the singlet field S_3 is decoupled from the doublet fields, and the MSSM mass matrix is recovered for the (S_1, S_2) system. This scenario indicates that, even for moderate λ and κ , m_h should change little from its MSSM prediction. So in order to show the difference of the two models in predicting m_h , we are more interested in large λ case. Especially we will mainly discuss $\lambda > M_Z/v \simeq 0.53$ case, where the tree level contributions to m_h^2 , i.e. \mathcal{M}_{22}^2 , are maximized for moderate values of $\tan \beta$ rather than by large values of $\tan \beta$ as in the MSSM.
- Scenario II: $\mathcal{M}_{11}^2 \gg \mathcal{M}_{22}^2 \gg \mathcal{M}_{12}^2$ and $(\mathcal{M}_{11}^2 - \mathcal{M}_{33}^2) \gg \mathcal{M}_{13}^2$, which can be easily realized for a large M_A^2 . In this limit, S_1 is decoupled from the (S_2, S_3) system and the properties of m_h can be qualitatively understood by the 2×2 matrix [15]

$$\tilde{M}^2 = \begin{pmatrix} \mathcal{M}_{22}^2 + \delta^2 & \mathcal{M}_{23}^2 \\ \mathcal{M}_{23}^2 & \mathcal{M}_{33}^2 - \Delta^2 \end{pmatrix}, \quad (14)$$

where δ^2 denotes the radiative corrections to m_h with its form given by the last two terms of Eq.(3), and Δ^2 represents the potentially important effect of (S_1, S_3) mixing on

\tilde{M}_{22}^2 . This matrix indicates that the (S_2, S_3) mixing can push m_h up once $\tilde{M}_{11}^2 > \tilde{M}_{22}^2$, and such effect is maximized for \tilde{M}_{11}^2 slightly larger than \tilde{M}_{22}^2 and at the same time $\tilde{M}_{12}^4 = \mathcal{M}_{23}^4$ slightly below $\tilde{M}_{11}^2 \tilde{M}_{22}^2$ (larger \tilde{M}_{12} will destabilize the vacuum) [15]. Obviously, in this push-up case, h is the next-to-lightest CP-even Higgs boson and the larger the (S_2, S_3) mixing is, the heavier h becomes. Alternatively, the mixing can pull m_h down on the condition of $\tilde{M}_{11}^2 < \tilde{M}_{22}^2$, which occurs for large $\kappa\mu$ (for $M_A \sin 2\beta/\mu \sim 2$, see discussion below) as indicated by the expression of \mathcal{M}_{33}^2 and the positiveness of Δ^2 . Here we remind that, due to the extra contribution $\lambda^2 v^2 \sin^2 2\beta$ to m_h^2 at tree level, m_h in the pull-down case may still be larger than its MSSM prediction for a certain δ^2 .

Since our results presented below is approximately described by scenario II, we now estimate the features of its favored region to predict $m_h \simeq 125\text{GeV}$. First, since $\tilde{M}_{11}^2 \sim \mathcal{O}(100^2)\text{GeV}^2$, $\mathcal{M}_{11}^2 \gg \mathcal{M}_{22}^2$ implies that $M_A \gtrsim \mathcal{O}(300)\text{GeV}$. Numerically, we find $M_A \gtrsim \mathcal{O}(300)\text{GeV}$ for the push-up case, and $M_A \gtrsim \mathcal{O}(500)\text{GeV}$ for the pull-down case (see Fig.7). Second, $\tilde{M}_{12}^2 = \mathcal{M}_{23}^2$ must be relatively small, which implies that $M_A \sin 2\beta/\mu \sim 2$ for $\lambda > 0.53$. This can be understood as follows. In the push-up case, since $\tilde{M}_{22}^2 < \tilde{M}_{11}^2 \sim \mathcal{O}(100^2)\text{GeV}^2$, the condition $\mathcal{M}_{23}^4 < \tilde{M}_{11}^2 \tilde{M}_{22}^2$ (for vacuum stability) has limited the size of \mathcal{M}_{23}^2 . While in the pull-down case, a very large \mathcal{M}_{23}^2 will suppress greatly m_h to make it difficult to reach 125GeV, and this in return limits the size of \mathcal{M}_{23}^2 . Given that $\mu \gtrsim 100\text{ GeV}$ as required by the LEP bound on chargino mass and that a larger μ is favored for the pull-down scenario, one can infer that the value of $M_A \sin 2\beta/\mu$ should be around 2 after considering that the third term in \mathcal{M}_{23}^2 is less important. Numerically speaking, we find $|\mathcal{M}_{23}^2/(2\lambda\mu v)| \leq 0.2$ and $1.4 \leq M_A \sin 2\beta/\mu \leq 2$ (see Fig.7). Lastly, light stops may be possible in the NMSSM with large λ to predict $m_h \simeq 125\text{GeV}$. To see this, we consider the parameters $\lambda = 0.7$ and $\tan\beta = 1.5$, and we get $\delta^2/125^2 \sim 5\%$ without considering the mixing effect to predict $m_h \simeq 125\text{GeV}$. This is in sharp contrast with $\delta^2/125^2 \sim 55\%$ in MSSM for $\tan\beta = 5$.

In this work we use the package NMSSMTools [20] to calculate the Higgs masses and mixings, which includes the dominant one-loop and leading logarithmic two-loop corrections to \mathcal{M}^2 . We checked our MSSM results of m_h by using the code FeynHiggs[21] and found the

results given by NMSSMTools and FeynHiggs are in good agreement (for $m_h \sim 125\text{GeV}$ they agree within 0.5GeV for same MSSM parameters).

III. NUMERICAL RESULTS AND DISCUSSIONS

In this work, we scan the parameters of the models and investigate the samples that predict $123\text{GeV} \leq m_h \leq 127\text{GeV}$ and at the same time survive the following constraints [20]: (1) The constraint from the LHC search channel $pp \rightarrow H \rightarrow 2\tau$ for non-standard Higgs boson. (2) The limits from the LEP and the Tevatron on the masses of sparticles as well as on the neutralino pair productions. (3) The constraints from B-physics, such as $B \rightarrow X_s \gamma$, the latest experimental result of $B_s \rightarrow \mu^+ \mu^-$, $B_d \rightarrow X_s \mu^+ \mu^-$, $B^+ \rightarrow \tau^+ \nu$ and the mass differences ΔM_d and ΔM_s . (4) The indirect constraints from the electroweak precision observables such as $\sin^2 \theta_{eff}^\ell$, ρ_ℓ and M_W , and their combinations $\epsilon_i (i = 1, 2, 3)$ [22]. We require ϵ_i to be compatible with the LEP/SLD data at 95% confidence level. We also require the SUSY prediction of the observable $R_b (\Gamma(Z \rightarrow b\bar{b})/\Gamma(Z \rightarrow \text{hadrons}))$ to be within the 2σ range of its experimental value [23]. (5) The constraints from the muon anomalous magnetic moment: $a_\mu^{exp} - a_\mu^{SM} = (25.5 \pm 8.2) \times 10^{-10}$ [24]. We require the SUSY effects to explain the discrepancy at 2σ level. (6) The dark matter constraints from WMAP relic density ($0.1053 < \Omega h^2 < 0.1193$) [25] and the direct search result from XENON100 experiment (at 90% C.L.) [26]. (7) For the NMSSM, we also require the absence of a Landau singularity below the GUT scale, which implies $\lambda \lesssim 0.7$ for small κ and $\kappa \lesssim 0.5$ for $\lambda > 0.53$ at weak scale. In our calculation, we fix $m_t = 172.9\text{ GeV}$ and $f_{Ts} = 0.02$ [27] (f_{Ts} denotes the strange quark fraction in the proton mass), and use the package NMSSMTools to implement most of the constraints and to calculate the observables we are interested in.

In our scan, we note that the soft parameters in the slepton sector can only affect significantly the muon anomalous magnetic moment a_μ , which will in return limit the important parameter $\tan \beta$, so we assume them a common value $m_{\tilde{l}}$ and treat it as a free parameter. For the soft parameters in the first two generation squark sector, due to their little effects on the properties of the Higgs bosons, we fix them to be 1 TeV. As for the gaugino masses, we assume the grand unification relation, $3M_1/5\alpha_1 = M_2/\alpha_2 = M_3/\alpha_3$ with α_i being the fine structure constants of the different gauge groups, and treat M_1 as a free parameter. In order to reduce free parameters, we also assume the unimportant parameters M_{D_3} and A_b

to satisfy $M_{D_3} = M_{U_3}$ and $A_b = A_t$.

A. Implication of $m_h \simeq 125\text{GeV}$ in generic SUSY

In order to study the implication of $m_h \simeq 125\text{GeV}$ in generic SUSY, we relax the soft mass parameters to 5 TeV and perform an extensive random scan over the following parameter regions:

$$\begin{aligned} 1 \leq \tan \beta \leq 60, \quad 90 \text{ GeV} \leq m_A \leq 1 \text{ TeV}, \quad 100 \text{ GeV} \leq \mu \leq 2 \text{ TeV}, \\ 100 \text{ GeV} \leq M_{Q_3}, M_{U_3} \leq 5 \text{ TeV}, \quad |A_t| \leq 5 \text{ TeV}, \\ 100 \text{ GeV} \leq m_{\tilde{t}} \leq 1 \text{ TeV}, \quad 50 \text{ GeV} \leq M_1 \leq 500 \text{ GeV}, \end{aligned} \quad (15)$$

for the MSSM, and

$$\begin{aligned} 0 < \lambda \leq 0.2, \quad 0 < \kappa \leq 0.7, \quad 90 \text{ GeV} \leq M_A \leq 1 \text{ TeV}, \quad |A_\kappa| \leq 1 \text{ TeV}, \\ 100 \text{ GeV} \leq M_{Q_3}, M_{U_3} \leq 5 \text{ TeV}, \quad |A_t| \leq 5 \text{ TeV}, \\ 1 \leq \tan \beta \leq 60, \quad 100 \text{ GeV} \leq \mu, m_{\tilde{t}} \leq 1 \text{ TeV}, \quad 50 \text{ GeV} \leq M_1 \leq 500 \text{ GeV}, \end{aligned} \quad (16)$$

for the NMSSM. In our scan, we only keep the samples satisfying the requirements listed in the text (including $123\text{GeV} \leq m_h \leq 127\text{GeV}$). To show the differences between the MSSM and the NMSSM, we also perform a scan similar to Eq.(16) except that we require $\lambda > m_Z/v \simeq 0.53$. In Fig.1, we show the correlation of the lighter top-squark mass ($m_{\tilde{t}_1}$) with the ratio X_t/M_S ($M_S = \sqrt{m_{\tilde{t}_1}m_{\tilde{t}_2}}$) for the surviving samples in the MSSM and NMSSM. As expected from Eq.(3), in order to predict $m_h \simeq 125\text{GeV}$ in the MSSM, a large X_t is needed for a moderate light \tilde{t}_1 , and with \tilde{t}_1 becoming heavy, the ratio X_t/M_S decreases, but is unlikely to vanish for $m_{\tilde{t}_1} < 5\text{TeV}$. These features are maintained for NMSSM with $\lambda \leq 0.2$ (see the middle panel) but changed for NMSSM with a large λ , where X_t can possibly vanish even for $m_{\tilde{t}_1} \sim 1\text{TeV}$. Fig.1 also shows that a \tilde{t}_1 as light as 200GeV is still able to give the required m_h . But in this case X_t is large ($X_t/\sqrt{m_{\tilde{t}_1}m_{\tilde{t}_2}} > \sqrt{6}$), which leads to a large mass splitting between two stops ($m_{\tilde{t}_2} \gg m_{\tilde{t}_1}$). Note that a \tilde{t}_1 as light as 200GeV does not contradict the recent SUSY search result of the LHC [28].

Since in heavy SUSY the radiative correction δ^2 is usually very large, $m_h \simeq 125\text{GeV}$ is unlikely to impose tight constraints on other parameters of the models. Considering heavy

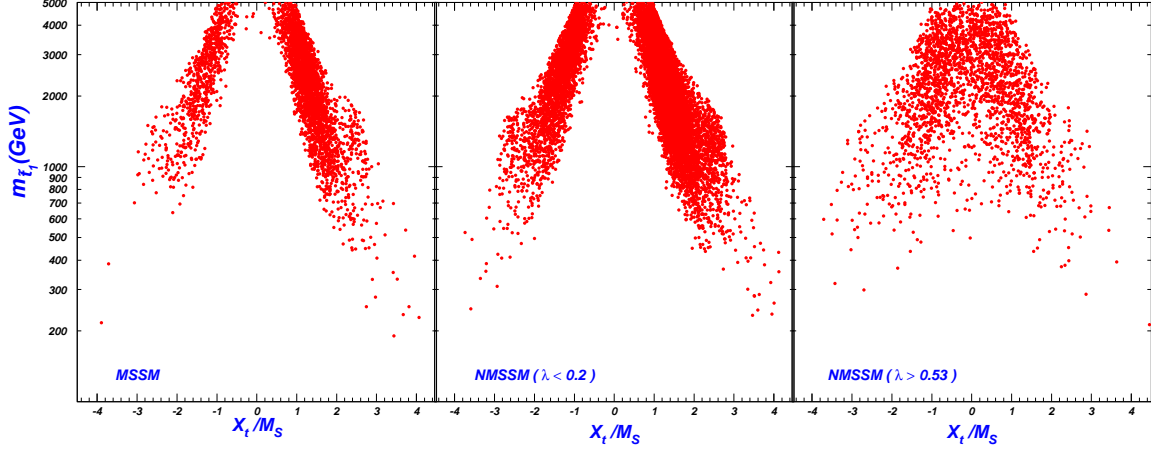


FIG. 1: The scatter plots of the samples in the MSSM and NMSSM satisfying all the requirements (1-7) listed in the text (including $123\text{GeV} \leq m_h \leq 127\text{GeV}$), projected in the plane of $m_{\tilde{t}_1}$ versus X_t/M_S with $M_S \equiv \sqrt{m_{\tilde{t}_1} m_{\tilde{t}_2}}$ and $X_t \equiv A_t - \mu \cot \beta$.

SUSY is disfavored by naturalness, we in the following concentrate on the implication of $m_h \simeq 125\text{GeV}$ in sub-TeV SUSY.

B. Implication of $m_h \simeq 125\text{GeV}$ in sub-TeV SUSY

In this section, we study the implication of $m_h \simeq 125\text{GeV}$ in low energy MSSM and NMSSM. In order to illustrate the new features of the NMSSM, we only consider the case with $\lambda > 0.53$. Our scans over the parameter spaces are quite similar to those in Eq.(15) and Eq.(16) except that we narrow the ranges of M_{Q_3} , M_{U_3} and A_t as follows:

$$100 \text{ GeV} \leq (M_{Q_3}, M_{U_3}) \leq 1 \text{ TeV}, \quad |A_t| \leq 3 \text{ TeV}. \quad (17)$$

In Fig.2 we project the surviving samples of the models in the plane of $m_{\tilde{t}_1}$ versus A_t , showing the results with $R_{\gamma\gamma} < 1$ and $R_{\gamma\gamma} > 1$ separately. As we analyzed in Sec. II, the SM-like Higgs in the NMSSM may be either the lightest Higgs boson (corresponding to the pull-down case) or the next-to-lightest Higgs boson (the push-up case). In the figure we distinguished these two cases. We note that among the surviving samples the number of the pull-down case is about twice the push-up case.

Fig.2 shows that, in order to get $m_h \simeq 125\text{GeV}$ in the MSSM, $m_{\tilde{t}_1}$ and $|A_t|$ must be larger than about 300GeV and 1.5TeV respectively, and the bounds are pushed up to 600GeV and 1.8TeV respectively for $R_{\gamma\gamma} > 1$. While in the NMSSM, a \tilde{t}_1 as light as about 100GeV (in

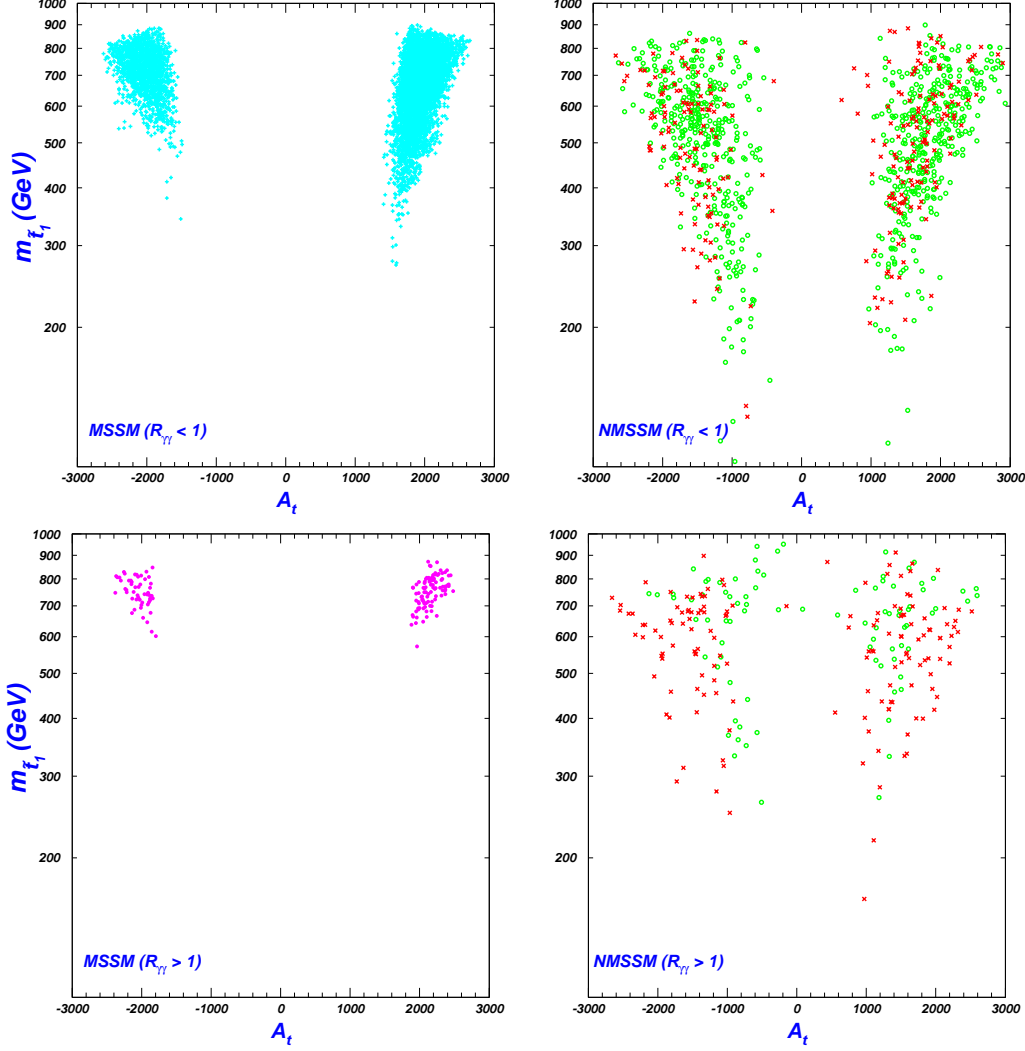


FIG. 2: Same as Fig.1, except that the samples are based on the narrowed scan ranges of the soft masses shown in Eq.(17) for both models and the requirement $\lambda > 0.53$ for the NMSSM. Here the samples are projected in the plane of $m_{\tilde{t}_1}$ versus A_t . The upper (lower) panels correspond to $R_{\gamma\gamma} < 1$ ($R_{\gamma\gamma} > 1$) with $R_{\gamma\gamma} \equiv \sigma_{SUSY}(pp \rightarrow h \rightarrow \gamma\gamma)/\sigma_{SM}(pp \rightarrow h \rightarrow \gamma\gamma)$. For the NMSSM results, the circles (green) denote the case of the lightest Higgs boson being the SM-like Higgs (the so-called pull-down case), and the times (red) denotes the case of the next-to-lightest Higgs boson being the SM-like Higgs (the so-called push-up case).

either the pull-down or push-up case) is still able to predict $m_h \simeq 125\text{GeV}$, and even if one require $R_{\gamma\gamma} > 1$, a \tilde{t}_1 as light as about 200GeV is allowed. The fact that the NMSSM allows a lighter \tilde{t}_1 than the MSSM indicates that the NMSSM is more natural than the MSSM in light of the LHC results.

Since a light \tilde{t}_1 may significantly change the effective couplings C_{hgg} and $C_{h\gamma\gamma}$, we present

TABLE I: The ranges of the rescaled couplings $C_{hgg} \equiv C_{hgg}^{\text{SUSY}}/C_{hgg}^{\text{SM}}$ and $C_{h\gamma\gamma} \equiv C_{h\gamma\gamma}^{\text{SUSY}}/C_{h\gamma\gamma}^{\text{SM}}$ predicted by the surviving samples of the two models. The region of $C_{hgg}(R_{\gamma\gamma} > 1)$ is obtained by only considering the samples with $R_{\gamma\gamma} > 1$.

	C_{hgg}	$C_{hgg}(R_{\gamma\gamma} > 1)$	$C_{h\gamma\gamma}$	$C_{h\gamma\gamma}(R_{\gamma\gamma} > 1)$
MSSM	$0.85 \sim 0.99$	$0.95 \sim 0.99$	$1 \sim 1.25$	$1.05 \sim 1.25$
NMSSM	$0.3 \sim 1$	$0.7 \sim 1$	$0.7 \sim 1.2$	$0.85 \sim 1.05$

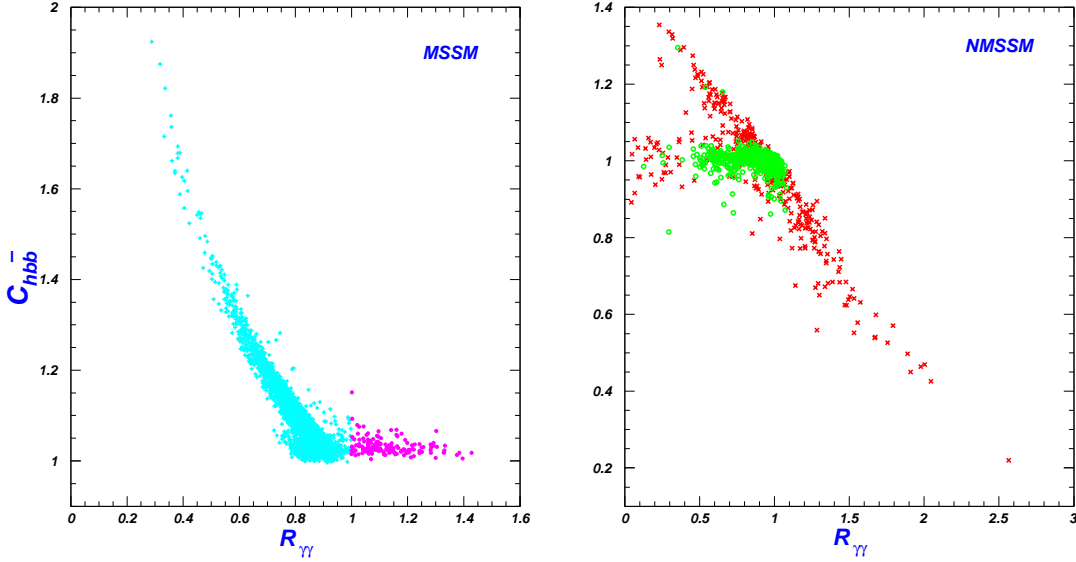


FIG. 3: Same as Fig.2, but showing the dependence of the di-photon signal rate $R_{\gamma\gamma}$ on the effective $h\bar{b}b$ coupling $C_{h\bar{b}b} \equiv C_{h\bar{b}b}^{\text{SUSY}}/C_{h\bar{b}b}^{\text{SM}}$.

in Table I their predicted ranges for the surviving samples. This table shows that C_{hgg} is always reduced, and for $m_{\tilde{t}_1} \sim 100\text{GeV}$ in the NMSSM, the reduction factor may reach 70%. While $C_{h\gamma\gamma}$ exhibits quite strange behaviors: it is enhanced in the MSSM, but may be either enhanced or suppressed in the NMSSM. This is because, unlike C_{hgg} which is affected only by squark loops, $C_{h\gamma\gamma}$ gets new physics contributions from loops mediated by charged Higgs boson, charginos, sleptons and also squarks, and there exists cancelation among different loops. As will be shown below, the current experiments can not rule out light sparticles like $\tilde{\tau}_1$ and chargino. Although the contributions of these particles to $C_{h\gamma\gamma}$ are far smaller than the W loop contribution, they may still alter the coupling significantly.

Since the di-photon signal is the most important discovery channel for the Higgs boson around 125GeV, it is useful to study its rate carefully. From Eq.(1) one can learn that the

rate is affected by C_{hgg} and $C_{h\gamma\gamma}$ discussed above, and also by the total width of h (or more basically by the $hb\bar{b}$ coupling since $b\bar{b}$ is the dominant decay of h). The importance of $hb\bar{b}$ coupling on the di-photon rate was recently emphasized in [6]. Here we restrict our study to the $m_h \simeq 125\text{GeV}$ case. In Fig.3 we show the dependence of the di-photon signal rate $R_{\gamma\gamma}$ on the effective $hb\bar{b}$ coupling (including the potentially large SUSY corrections [6, 29]) normalized by its SM value. This figure indicates that although the rate is suppressed for most of the surviving samples in both models, there still exist some samples with enhanced rate, especially the NMSSM is more likely to push up the rate than the MSSM. This feature can be understood as follows. In SUSY, $R_{\gamma\gamma} > 1$ requires approximately the combination $C_{hgg}C_{h\gamma\gamma}/C_{hb\bar{b}}$ to exceed 1. For the MSSM, given $C_{hgg} < 1$ and $C_{hb\bar{b}} \geq 1$ for nearly all the cases, this condition is not easy to satisfy. While in the NMSSM, due to the mixing between the doublet field S_2 and the singlet field S_3 , $C_{hb\bar{b}} < 1$ is possible once the singlet component in h is significant, which is helpful to enhance the combination. In fact, we analyzed carefully the $R_{\gamma\gamma} > 1$ cases and found they are characterized by $C_{hgg}, C_{hb\bar{b}} \simeq 1$ and $C_{h\gamma\gamma} > 1$ in the MSSM, and by $C_{hb\bar{b}} < 1$ in the NMSSM. In other words, it is the enhanced $h\gamma\gamma$ coupling (reduced total width of h) that mainly push up the di-photon rate in the MSSM (NMSSM) to exceed its SM prediction. Fig.3 also indicates that the pull-down case in the NMSSM is less effective in reducing $C_{hb\bar{b}}$ and thus can hardly enhance the di-photon rate. This is because in the push-up case, both \tilde{M}_{11}^2 and \tilde{M}_{22}^2 in Eq.(14) are moderate and often comparable, which are helpful to enhance the (S_2, S_3) mixing. Finally, we note that in some rare cases of the NMSSM the ratio $R_{\gamma\gamma}$ may be very small even for $C_{hb\bar{b}} < 1$. This is because there exists very light Higgs boson so that h decays dominantly into them.

In order to further clarify the reason for the enhancement of the di-photon rate in the MSSM, we scrutinize carefully the parameters of the model and find that the samples with $R_{\gamma\gamma} > 1$ correspond to the case with a large $\mu \tan \beta$ and $m_{\tilde{\tau}_1} < 200\text{GeV}$, which is illustrated in Fig.4. This means that the stau loop plays an important role in enhancing $C_{\gamma\gamma}$. We note that similar conclusion was recently achieved in [18], but in that work the authors did not consider the tight experimental constraints. From Fig.4 we also note that $R_{\gamma\gamma} < 0.95$ is predicted in the MSSM with $m_{\tilde{\tau}_1} > 250\text{GeV}$. So future precise measurement of $R_{\gamma\gamma}$ and $m_{\tilde{\tau}_1}$ may be utilized to verify the correctness of the MSSM.

Considering the process $pp \rightarrow h \rightarrow VV^*$ ($V = W, Z$) is another important Higgs search channel, we in Fig.5 show the signal rate versus the hVV coupling. This figure shows that

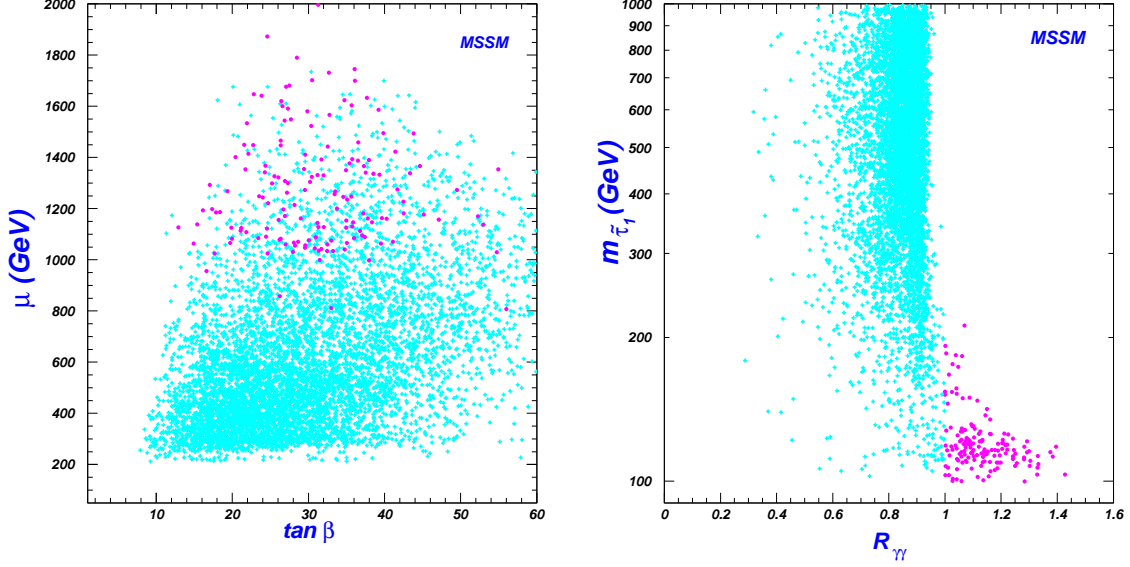


FIG. 4: Same as Fig.2, but only for the MSSM, projected in the planes of $\tan\beta$ versus μ and $R_{\gamma\gamma}$ versus $m_{\tilde{\tau}_1}$.

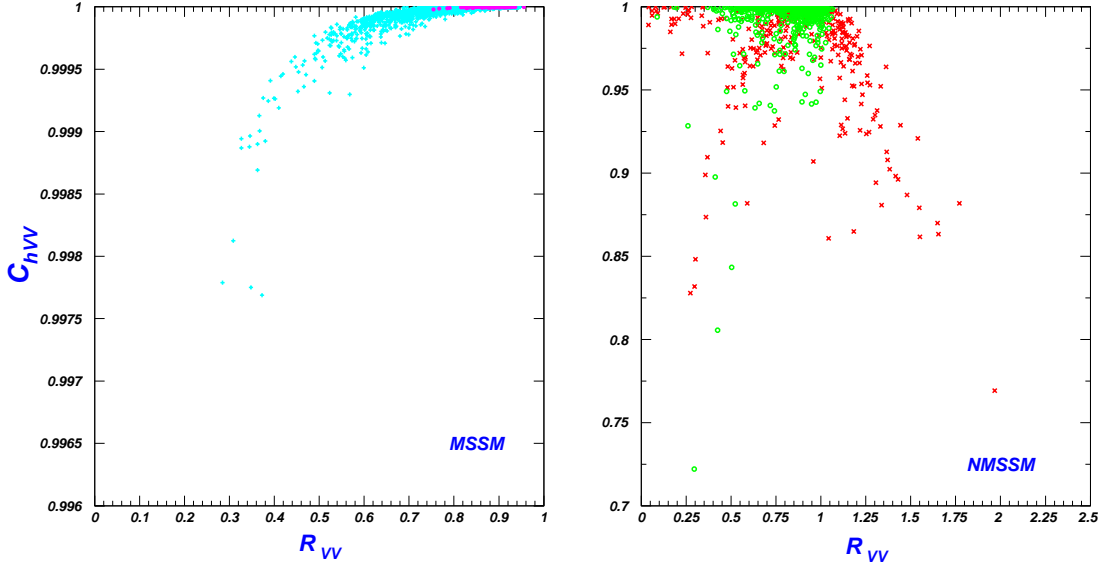


FIG. 5: Same as Fig.2, but showing the signal rate $R_{VV} \equiv \sigma_{\text{SUSY}}(pp \rightarrow h \rightarrow VV^*)/\sigma_{\text{SM}}(pp \rightarrow h \rightarrow VV^*)$ versus the coupling $C_{hVV} \equiv C_{hVV}^{\text{SUSY}}/C_{hVV}^{\text{SM}}$.

in the MSSM, h is highly SM-like, while in the NMSSM, the singlet component in h may be sizable, especially in the push-up case, so that C_{hVV} is reduced significantly. The signal rate R_{VV} also behaves differently in the two models. In the MSSM, because $C_{hgg} < 1$ and in most cases $C_{hbb} > 1$, R_{VV} is always less than 1 (for $R_{\gamma\gamma} > 1$ it varies between 0.7 and 0.95). In the NMSSM, however, R_{VV} may exceed 1 and in this case we find $R_{VV} \simeq R_{\gamma\gamma}$. The reason

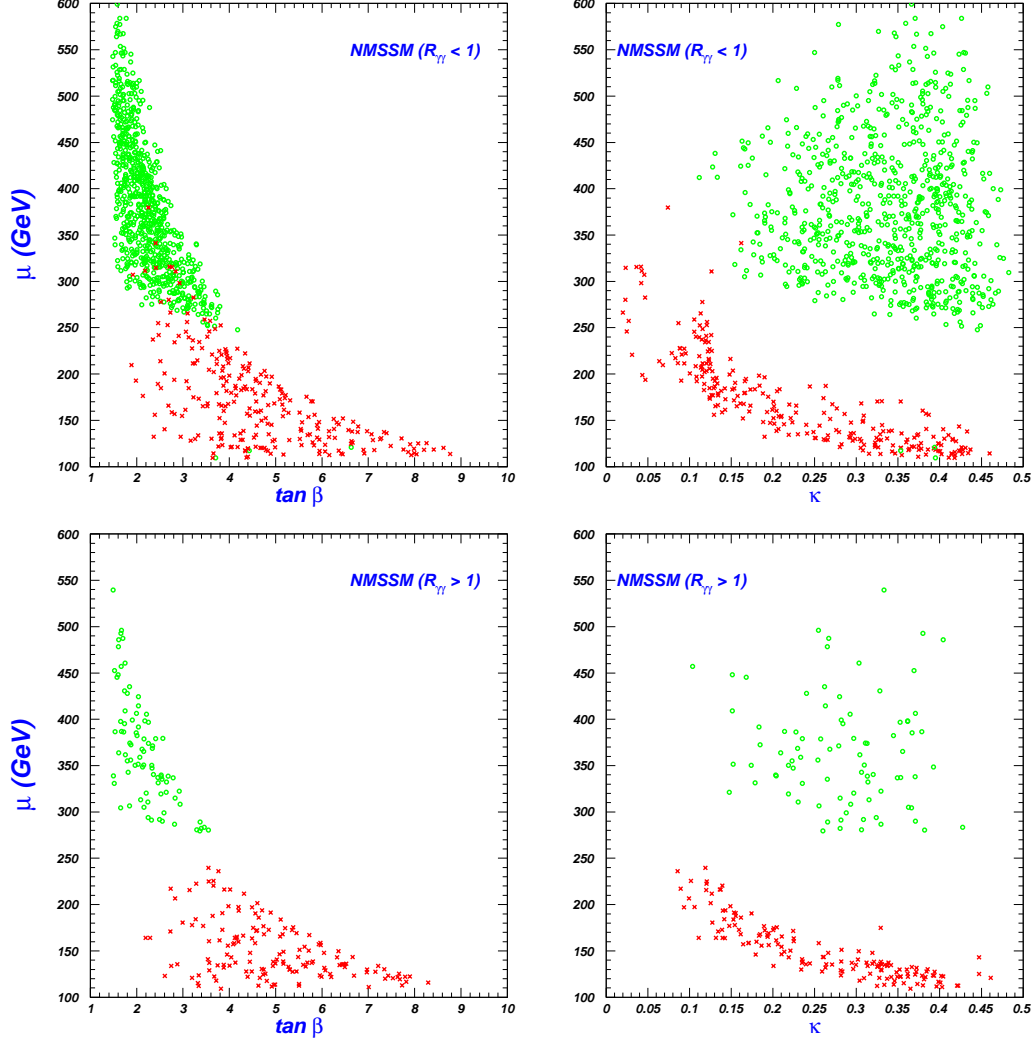


FIG. 6: Same as Fig.2, but projected in the planes of μ versus $\tan\beta$ and versus κ respectively.

for such a correlation is the two quantities have the same origin for their enhancement, i.e. the suppression of the $hb\bar{b}$ due to the presence of the singlet component in h .

Next we investigate the favored parameter space of the NMSSM to predict $m_h \simeq 125\text{GeV}$. As introduced in Sec. II, besides the soft parameters in the stop sector, the sensitive parameters include $\tan\beta$, μ , κ as well as M_A . In Fig.6, we project the surviving samples in the planes of μ versus $\tan\beta$ and versus κ . This figure shows three distinctive characters for the allowed parameters. The first is that $\tan\beta$ must be moderate, below 4 and 9 for the pull-down and the push-up case, respectively. Two reasons can account for it. One is that in the NMSSM with large λ , the precision electroweak data, i.e. the constraint (4), strongly disfavor a large $\tan\beta$ [30]. The other reason is that, as far as $\lambda > 0.53$ is concerned, a

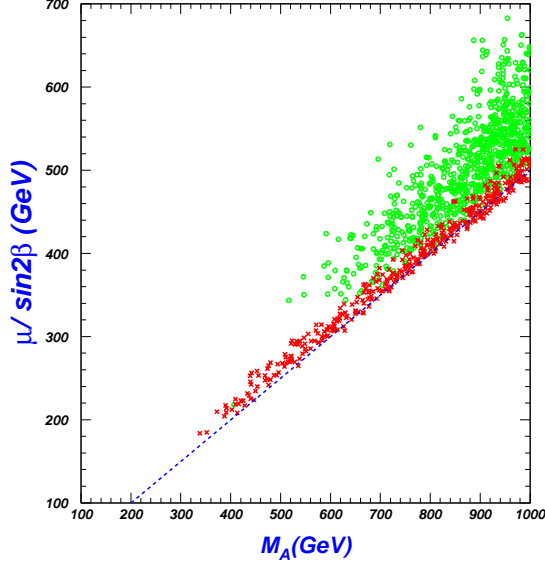


FIG. 7: Same as Fig.6, but showing the correlation between M_A and $\mu/\sin 2\beta$. The dashed line denotes the relation $M_A \sin 2\beta/\mu = 2$.

moderate $\tan\beta$ is welcomed to enhance the tree level value of m_h^2 (i.e. \mathcal{M}_{22}^2) so that even without heavy stops, m_h can still reach 125GeV. Moreover, since the (S_2, S_3) mixing is to reduce the value of \tilde{M}_{11}^2 in Eq.(14) in the pull-down case, a larger \tilde{M}_{22}^2 (or equivalently a smaller $\tan\beta$) is favored by the Higgs mass. The second character is that $\kappa\mu$ in the push-up case is usually much smaller than that in the pull-down case. This is because, as we introduced in Sec. II, a large $\kappa\mu$ is needed by the pull-down case to enhance \tilde{M}_{22}^2 in Eq.(14). The third character is obtained by comparing the parameter regions in the upper panels with those in the lower panels, which shows that $R_{\gamma\gamma} > 1$ puts a lower bound on κ , i.e. $\kappa \gtrsim 0.1$. The underlying reason is that for $\kappa < 0.1$, the dark matter will be light and singlino-like, and to get its currently measured relic density, the dark matter must annihilate in the early universe by exchanging a light Higgs boson [31]. In this case, h mainly decays into the light bosons, which in return will suppress the di-photon rate.

In Fig.7 we show the correlation of M_A with $\mu/\sin 2\beta$. This figure indicates that $M_A \gtrsim 300\text{GeV}$ for the push-up case and $M_A \gtrsim 500\text{GeV}$ for the pull-down case, which is in agreement with our expectation. In fact, we checked each surviving sample and found it satisfies the condition: $M_A^2 \gg \mathcal{M}_{22}^2 \gg \mathcal{M}_{12}^2$ and $(M_A^2 - \mathcal{M}_{33}^2) \gg \mathcal{M}_{13}^2$, so the samples can be well described by scenario II. We also checked that the mixing of the field S_1 with S_2/S_3 is small and M_A is approximately the heaviest CP-even Higgs boson mass. Fig.7 also

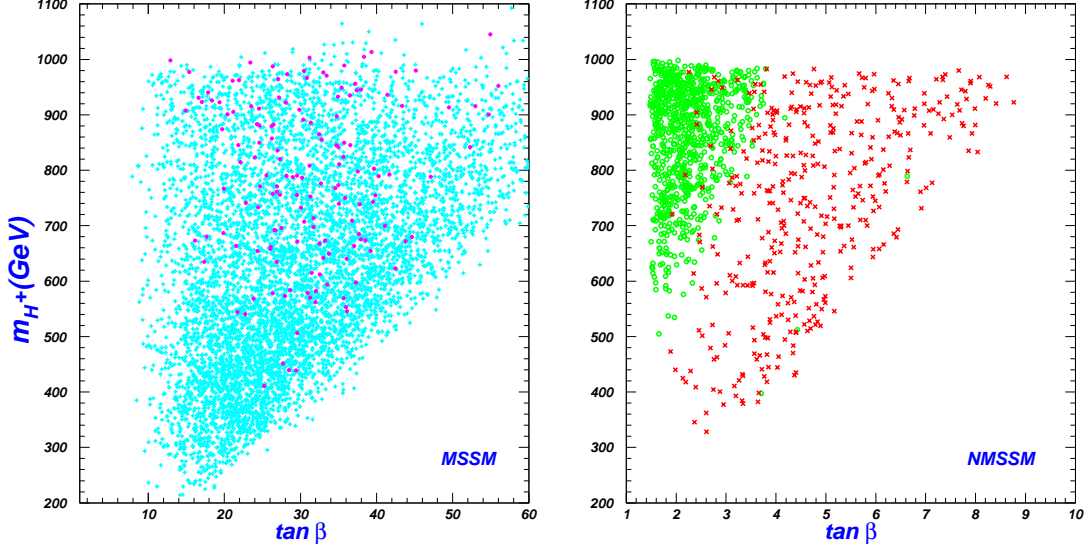


FIG. 8: Same as Fig.5, but projected on the plane of the charged Higgs boson mass and $\tan \beta$.

indicates that the relation $M_A \sin 2\beta/\mu = 2$ is maintained quite well in the push-up case, but is moderately spoiled in the pull-down case. The reason is, as we introduced in Sec. II, the requirement that \mathcal{M}_{23}^2 should be moderately small actually implies $C_A \sim 0$ with $C_A = 1 - (\frac{M_A \sin 2\beta}{2\mu})^2 - \frac{\kappa}{2\lambda} \sin 2\beta$. In the push-up case the third term in C_A is not important, while in the pull case, although it is several times smaller than the second term, it may not be negligible. We checked our results and found $|C_A| \lesssim 0.2$ and $1.4 \lesssim M_A \sin 2\beta/\mu \lesssim 2$ for all the surviving samples.

About the NMSSM with $\lambda > 0.53$, three points should be noted. The first is, from the results presented in Fig.6, one may find the presence of a smuon and/or a chargino lighter than 250GeV. This is because the surviving samples are characterized either by $\tan \beta < 4$ or $\mu < 250\text{GeV}$ or by both in the NMSSM (see Fig.6). Then to explain the discrepancy of muon anomalous magnetic moment $m_{\tilde{\mu}} \leq 250\text{GeV}$ is needed for a low $\tan \beta$, and $m_{\tilde{\chi}^\pm} \simeq \mu$ implies $m_{\tilde{\chi}^\pm} \leq 250\text{GeV}$. We numerically checked the validity of this conclusion. The second point is, although $M_A \sin 2\beta/\mu \simeq 2$ may be regarded as a new source of fine tuning in the NMSSM, it is rather predictive to get the value of M_A once μ and $\tan \beta$ are experimental determined. Finally, we note the favored region for μ and $\tan \beta$ shown in Fig.6 does not overlap with that in Fig.4. This may be used to discriminate the models.

Finally, we briefly describe other implications of $m_h \simeq 125\text{GeV}$ in the SUSY models. In Fig.8 we project the surviving samples on the plane of $\tan \beta$ versus m_{H^+} with H^+ denoting the charged Higgs boson. This figure shows that H^+ must be heavier than about 200GeV

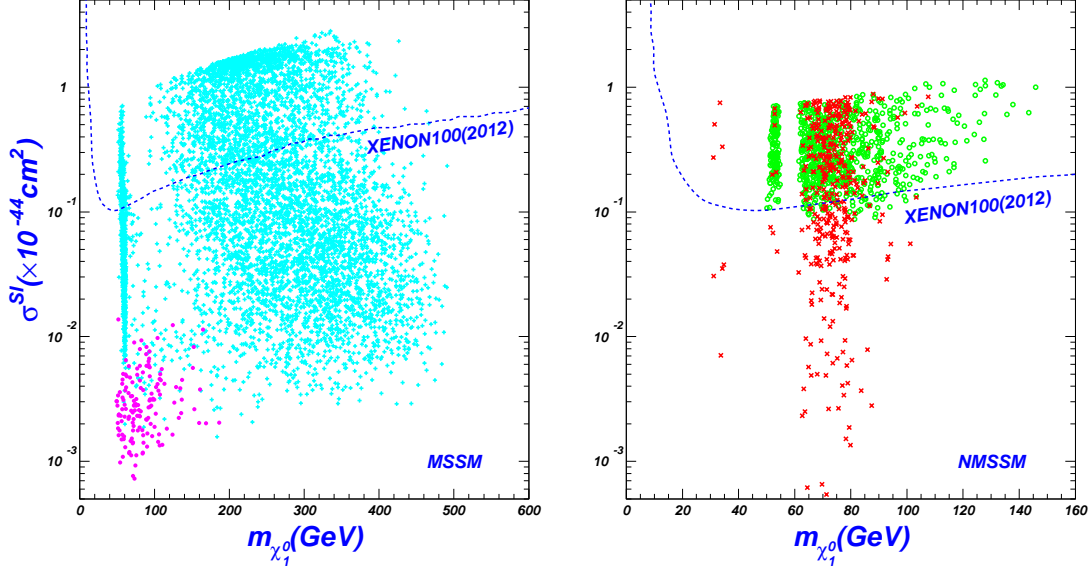


FIG. 9: Same as Fig.2, but exhibiting the spin-independent χ -nucleon scattering cross section as a function of the dark matter mass.

in the MSSM. This bound is much higher than the corresponding LEP bound, which is about 80GeV. For the NMSSM with a large λ , the bound can be further pushed up to about 300GeV. This figure also indicates that in the MSSM, $\tan\beta$ may reach 35 for $m_{H^+} = 400\text{GeV}$. Then based on the MC simulation by the ATLAS collaboration [32], one may expect that the charged Higgs may be observable from the process $pp \rightarrow tH^- \rightarrow bW\tau\nu_\tau$ at the early stage of the LHC. However, this may be impossible. The reason is, for relatively light H^+ and large $\tan\beta$, μ must be large to satisfy the constraint from dark matter direct detection experiments such as XENON100. This will greatly suppress the $\bar{t}bH^+$ coupling [33]. For the NMSSM, the hope to observe H^+ is also dim because $\tan\beta$ is small.

In Fig.9 we show the spin-independent elastic scattering between dark matter and nucleon. We use the formula presented in the Appendix of [34] to calculate the scattering rate. As expected, the XENON100 (2012) data to be released in near future will further exclude some samples, especially the pull-down case of the NMSSM will be strongly disfavored if XENON100 (2012) fails to find any evidence of dark matter (assuming the grand unification relation of the gaugino mass). From the left of Fig.9 one can learn that for the samples with $R_{\gamma\gamma} > 1$ in the MSSM, the scattering rate is small, usually at least one order below than the sensitivity of the XENON100 (2012).

IV. CONCLUSION

Motivated by the recent LHC hints of a Higgs boson around 125 GeV, we assume a SM-like Higgs with the mass 123-127 GeV and study its implication in low energy SUSY by comparing the MSSM and NMSSM. Under various experimental constraints at 2σ level (including the muon $g - 2$ and the dark matter relic density), we scanned over the parameter space of each model. Then in the parameter space allowed by current experimental constraints and also predicting a SM-like Higgs in 123-127 GeV, we examined the properties of the sensitive parameters and calculated the rates of the di-photon signal and the VV^* ($V = W, Z$) signals at the LHC. Among our various findings the typical ones are: (i) In the MSSM the top squark and A_t must be large and thus incur some fine-tuning, which can be much ameliorated in the NMSSM; (ii) In the MSSM a light $\tilde{\tau}$ is needed to make the di-photon rate of the SM-like Higgs exceed its SM prediction, while the NMSSM has more ways in doing this; (iii) In the MSSM the signal rates of $pp \rightarrow h \rightarrow VV^*$ at the LHC are never enhanced compared with their SM predictions, while in the NMSSM they may be enhanced; (iv) A large part of the parameter space so far survived will be soon covered by the expected XENON100(2012) sensitivity (especially for the NMSSM).

Therefore, although the low energy SUSY can in general accommodate a SM-like Higgs boson near 125 GeV and enhance its di-photon signal rate at the LHC, not all models of low energy SUSY are equally competent if they are required to satisfy all current experimental constraints. From our present study and some other studies in the literature, we conclude:

- The fancy CMSSM/mSUGRA is hard to give a 125 GeV SM-like Higgs boson [17].
- The MSSM can give such a 125 GeV Higgs and can also enhance its di-photon signal rate at the LHC, which, however, will incur some fine-tuning.
- The nMSSM (the nearly minimal SUSY model) can give a 125 GeV SM-like Higgs, but severely suppress its di-photon signal rate at the LHC [6].
- The NMSSM is so far the best model to accommodate such a 125 GeV Higgs; it can naturally (without fine-tuning) predict such a SM-like Higgs mass and readily enhance its di-photon signal rate at the LHC. At the same time, in a large part of its parameter space, this model can also enhance the signal rates $pp \rightarrow h \rightarrow VV^*$ ($V = Z, W$) at the

LHC and predict a large scattering rate of dark matter and nucleon at the XENON100. So the interplay of LHC and XENON100 will soon allow for a good test of this model.

Acknowledgement

This work was supported in part by the National Natural Science Foundation of China (NNSFC) under grant Nos. 10821504, 11135003, 10775039, 11075045, by Specialized Research Fund for the Doctoral Program of Higher Education with grant No. 20104104110001, and by the Project of Knowledge Innovation Program (PKIP) of Chinese Academy of Sciences under grant No. KJCX2.YW.W10.

-
- [1] ATLAS Collaboration, arXiv:1202.1408 [hep-ex]; arXiv:1202.1414 [hep-ex]; arXiv:1202.1415 [hep-ex].
 - [2] CMS Collaboration, arXiv:1202.1416 [hep-ex]; arXiv:1202.1487 [hep-ex]; arXiv:1202.1488 [hep-ex]; arXiv:1202.1489 [hep-ex]; arXiv:1202.1997 [hep-ex]; arXiv:1202.3478 [hep-ex]; arXiv:1202.3617 [hep-ex]; arXiv:1202.4083 [hep-ex]; arXiv:1202.4195 [hep-ex].
 - [3] D. Carmi, A. Falkowski, E. Kuflik and T. Volansky, arXiv:1202.3144 [hep-ph].
 - [4] J. R. Espinosa, C. Grojean, M. Muhlleitner and M. Trott, arXiv:1202.3697 [hep-ph]; A. Azarov, R. Contino and J. Galloway, arXiv:1202.3415 [hep-ph].
 - [5] S. Moretti and S. Munir, Eur. Phys. J. C **47**, 791 (2006); K. Hsieh and C. P. Yuan, Phys. Rev. D **78**, 053006 (2008); I. Low and S. Shalgar, JHEP **0904**, 091 (2009); U. Ellwanger, Phys. Lett. B **698**, 293 (2011).
 - [6] J. Cao, Z. Heng, T. Liu, J. M. Yang, Phys. Lett. B **703**, 462 (2011).
 - [7] U. Ellwanger, arXiv:1112.3548.
 - [8] H. E. Haber and G. L. Kane, Phys. Rept. **117**, 75 (1985); J. F. Gunion and H. E. Haber, Nucl. Phys. B **272**, 1 (1986) [Erratum-ibid. B **402**, 567 (1993)].
 - [9] A. Djouadi, Phys. Rept. **459**, 1 (2008) [arXiv:hep-ph/0503173].
 - [10] M. S. Carena, J. R. Espinosa, M. Quiros and C. E. M. Wagner, Phys. Lett. B **355**, 209 (1995) [arXiv:hep-ph/9504316].
 - [11] P. H. Chankowski, J. R. Ellis and S. Pokorski, Phys. Lett. B **423**, 327 (1998) [hep-ph/9712234];

- R. Barbieri and A. Strumia, Phys. Lett. B **433**, 63 (1998) [hep-ph/9801353]; G. L. Kane and S. F. King, Phys. Lett. B **451**, 113 (1999) [hep-ph/9810374].
- [12] U. Ellwanger, C. Hugonie and A. M. Teixeira, Phys. Rept. **496**, 1 (2010); M. Maniatis, Int. J. Mod. Phys. **A25** (2010) 3505 [arXiv:0906.0777 [hep-ph]].
- [13] For phenomenological studies, see, e.g., J. R. Ellis *et al.*, Phys. Rev. D **39**, 844 (1989); M. Drees, Int. J. Mod. Phys. **A4**, 3635 (1989); S. F. King, P. L. White, Phys. Rev. D **52**, 4183 (1995); B. Ananthanarayan, P.N. Pandita, Phys. Lett. B **353**, 70 (1995); B. A. Dobrescu, K. T. Matchev, JHEP **0009**, 031 (2000); R. Dermisek, J. F. Gunion, Phys. Rev. Lett. **95**, 041801 (2005); G. Hiller, Phys. Rev. D **70**, 034018 (2004); F. Domingo, U. Ellwanger, JHEP **0712**, 090 (2007); Z. Heng *et al.*, Phys. Rev. D **77**, 095012 (2008); R. N. Hodgkinson, A. Pilaftsis, Phys. Rev. D **76**, 015007 (2007); W. Wang *et al.*, Phys. Lett. B **680**, 167 (2009); J. M. Yang, Int. J. Mod. Phys. D **20**, 1383 (2011) [arXiv:1102.4942 [hep-ph]]; U. Ellwanger and C. Hugonie, Mod. Phys. Lett. A **22**, 1581 (2007) [arXiv:hep-ph/0612133]; Eur. Phys. J. C **25**, 297 (2002) [arXiv:hep-ph/9909260]; U. Ellwanger, Eur. Phys. J. C **71**, 1782 (2011) [arXiv:1108.0157 [hep-ph]].
- [14] S. F. King, M. Muhlleitner and R. Nevzorov, arXiv:1201.2671 [hep-ph].
- [15] Z. Kang, J. Li and T. Li, arXiv:1201.5305 [hep-ph].
- [16] M. Bastero-Gil, C. Hugonie, S. F. King, D. P. Roy and S. Vempati, Phys. Lett. B **489**, 359 (2000) [hep-ph/0006198]; A. Delgado, C. Kolda, J. P. Olson and A. de la Puente, Phys. Rev. Lett. **105**, 091802 (2010) [arXiv:1005.1282 [hep-ph]]; U. Ellwanger, G. Espitalier-Noel and C. Hugonie, JHEP **1109** (2011) 105 [arXiv:1107.2472 [hep-ph]]; G. G. Ross and K. Schmidt-Hoberg, arXiv:1108.1284 [hep-ph].
- [17] S. Heinemeyer, O. Stal and G. Weiglein, arXiv:1112.3026; A. Arbey *et al.*, arXiv:1112.3028; L. J. Hall, D. Pinner and J. T. Ruderman, arXiv:1112.2703; P. Draper *et al.*, arXiv:1112.3068; A. Arbey, M. Battaglia and F. Mahmoudi, arXiv:1112.3032; O. Buchmueller *et al.*, arXiv:1112.3564; M. Kadastik *et al.*, arXiv:1112.3647; J. Cao, Z. Heng, D. Li and J. M. Yang, arXiv:1112.4391 [hep-ph]. A. Arvanitaki and G. Villadoro, arXiv:1112.4835 [hep-ph]; H. Baer, V. Barger, A. Mustafayev, arXiv:1112.3017; I. Gogoladze, Q. Shafi and C. S. Un, arXiv:1112.2206 [hep-ph]; J. L. Feng, K. T. Matchev and D. Sanford, arXiv:1112.3021 [hep-ph]; S. Akula, B. Altunkaynak, D. Feldman, P. Nath and G. Peim, arXiv:1112.3645 [hep-ph]; A. Bottino, N. Fornengo and S. Scopel, arXiv:1112.5666 [hep-ph].

- ph]; J. F. Gunion, Y. Jiang and S. Kraml, arXiv:1201.0982 [hep-ph]; P. Fileviez Perez, arXiv:1201.1501 [hep-ph]; J. Ellis, M. K. Gaillard and D. V. Nanopoulos, arXiv:1201.6045 [hep-ph]; N. Karagiannakis, G. Lazarides and C. Pallis, arXiv:1201.2111 [hep-ph]; L. Roszkowski, E. M. Sessolo and Y. -L. S. Tsai, arXiv:1202.1503 [hep-ph]; L. Aparicio, D. G. Cerdeno and L. E. Ibanez, arXiv:1202.0822 [hep-ph]; C. -F. Chang, K. Cheung, Y. -C. Lin and T. -C. Yuan, arXiv:1202.0054 [hep-ph]; K. A. Olive, arXiv:1202.2324 [hep-ph]; J. Ellis and K. A. Olive, arXiv:1202.3262 [hep-ph]; H. Baer, V. Barger and A. Mustafayev, arXiv:1202.4038 [hep-ph]; D. Ghosh, M. Guchait and D. Sengupta, arXiv:1202.4937 [hep-ph]; N. Desai, B. Mukhopadhyaya and S. Niyogi, arXiv:1202.5190 [hep-ph].
- [18] M. Carena, S. Gori, N. R. Shah and C. E. M. Wagner, arXiv:1112.3336 [hep-ph].
- [19] D. J. . Miller, R. Nevzorov and P. M. Zerwas, Nucl. Phys. B **681**, 3 (2004) [arXiv:hep-ph/0304049].
- [20] U. Ellwanger, J. F. Gunion and C. Hugonie, JHEP **0502**, 066 (2005); U. Ellwanger and C. Hugonie, Comput. Phys. Commun. **175**, 290 (2006).
- [21] G. Degrandi *et al.*, Eur. Phys. J. C **28** (2003) 133; S. Heinemeyer, W. Hollik and G. Weiglein, Eur. Phys. J. C **9** (1999) 343; S. Heinemeyer, W. Hollik and G. Weiglein, Comput. Phys. Commun. **124** (2000) 76; M. Frank *et al.*, JHEP **0702** (2007) 047;
- [22] G. Altarelli and R. Barbieri, Phys. Lett. B **253**, 161 (1991); M. E. Peskin, T. Takeuchi, Phys. Rev. D **46**, 381 (1992).
- [23] J. Cao and J. M. Yang, JHEP **0812**, 006 (2008).
- [24] M. Davier *et al.*, Eur. Phys. J. C **66**, 1 (2010).
- [25] J. Dunkley *et al.* [WMAP Collaboration], Astrophys. J. Suppl. **180**, 306 (2009).
- [26] E. Aprile *et al.* [XENON100 Collaboration], Phys. Rev. Lett. **107**, 131302 (2011).
- [27] H. Ohki *et al.*, Phys. Rev. D **78**, 054502 (2008); D. Toussaint and W. Freeman, Phys. Rev. Lett. **103**, 122002 (2009); J. Giedt, A. W. Thomas and R. D. Young, Phys. Rev. Lett. **103**, 201802 (2009).
- [28] N. Desai and B. Mukhopadhyaya, arXiv:1111.2830 [hep-ph]; X. J. Bi, Q. S. Yan and P. F. Yin, Phys. Rev. D **85**, 035005 (2012) [arXiv:1111.2250 [hep-ph]]; B. He, T. Li, Q. Shafi, arXiv:1112.4461 [hep-ph].
- [29] M. S. Carena, D. Garcia, U. Nierste and C. E. M. Wagner, Nucl. Phys. B **577**, 88 (2000).
- [30] J. Cao and J. M. Yang, Phys. Rev. D **78**, 115001 (2008).

- [31] J. Cao, H. E. Logan and J. M. Yang, Phys. Rev. D **79**, 091701 (2009).
- [32] G. Aad *et al.* [The ATLAS Collaboration], arXiv:0901.0512 [hep-ex].
- [33] J. Cao, *et al.*, Phys. Rev. D **82**, 051701 (2010).
- [34] J. Cao, *et al.*, JHEP **1007**, 044 (2010).